ISSN 1070-3632, Russian Journal of General Chemistry, 2006, Vol. 76, No. 3, pp. 335–339. © Pleiades Publishing, Inc., 2006.
Original Russian Text © I.A. Zvereva, Yu.E. Smirnov, T.Palstra, 2006, published in Zhurnal Obshchei Khimii, 2006, Vol. 76, No. 3, pp. 353–358.

Cation Distribution and Interatomic Interactions in Oxides with Heterovalent Isomorphism: X.[1] Structure of the $Ho_2SrAl_2O_7$ Oxide at 100, 298, and 673 K

I. A. Zvereva*, Yu. E. Smirnov*, and T. Palstra**

* *St. Petersburg State University, Universitetskii pr. 7, St. Petersburg, 198504 Russia*
** *Materials Science Center, University of Groningen, Netherlands*

Received June 22, 2005

Abstract — Crystallochemical data for the $Ho_2SrAl_2O_7$ oxide at 100, 293, and 673 K were obtained by full-profile X-ray analysis. Analysis of the thermal expansion anisotropy showed that increased temperature gives rise to equalization of metal–oxygen bond lengths in all oxygen polyhedra at the expense of lengthening of some bonds and virtual invariability of others.
DOI: 10.1134/S1070363206030017

The complex aluminate $Ho_2SrAl_2O_7$ crystallizing in the $Sr_3Ti_2O_7$ structural type (space group *I*4/*mmm*) is nowadays the last synthesized member of the $Ln_2 \cdot SrAl_2O_7$ lanthanide series. The first obtained were oxides containing La, Nd, and Gd were [2, 3]. Recently this series of aluminates was extended by oxides containing Sm, Eu, Dy, Tb, and Ho [4]. The preparation of single-phase samples of the second half of the lanthanide series was favored to a considerable extent by the research into the mechanism and kinetics of phase formation for four $Ln_2SrAl_2O_7$ aluminates (Ln = La, Nd, Sm, Gd) [5–7].

Compounds of this type belong to Ruddlesden–Popper phases [8], which are constructed by the block principle from intergrowing perovskite (P) and rock-salt (RS) layers alternating as ...(P)(P)(RS)(P)(P)(RS)... . In the $Ln_2SrAL_2O_7$ structure, isomorphic Ln^{+3} and Sr^{+2} cations fill, with various probability, two sites: 2*b* and 4*e* centers of oxygen polyhedra with the coordination numbers 12 and 9, i.e. $(Ln,Sr)O_{12}$ cubic octahedra and $(Ln,Sr)O_9$ single-cap distorted tetragonal antiprisms (Fig. 1). It is commonly accepted that the first of them are in the perovskite double layers (P)(P), and the second, in the rock-salt layers. Data on interatomic distances and distribution of rare-earth metal cations over two sites in the $Ln_2SrAl_2O_7$ aluminates (Ln = La–Ho) we obtained earlier by means of full-profile X-ray analysis at room temperature [4, 9]. It was found that the probability of filling with Sr^{+2} cations of the $(Ln,Sr)O_{12}$ oxygen cubic octahedra and with Ln^{+3} cations of the nine-vertex $(Ln,Sr)O_9$ polyhedra increases in the La–Ho series. These conclusions were drawn on the basis of directly calculated population densities of the structural sites and trends in variation of metal–oxygen bond lengths. The structure of $Gd_2SrAl_2O_7$ was also studied at 1273 K [10]. The resulting crystallographic data gave

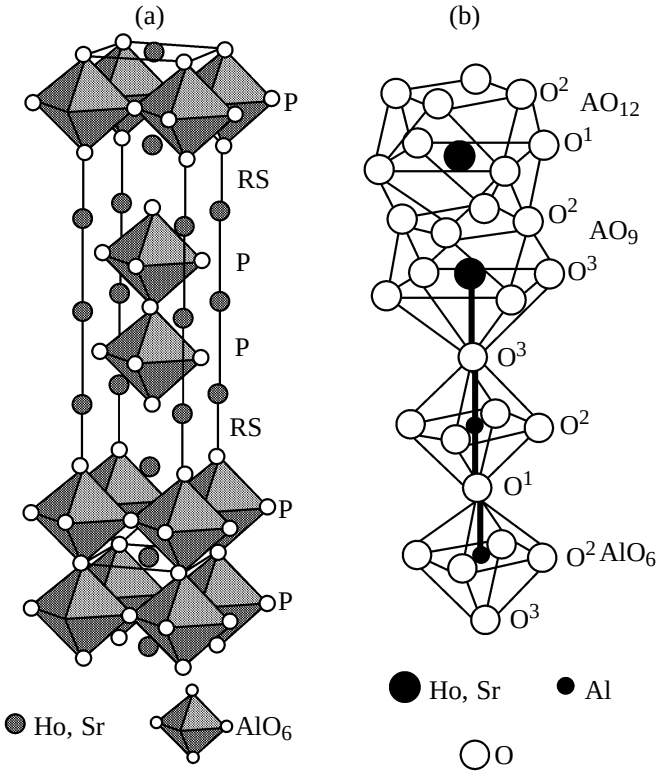

Fig. 1. (a) Unit cell and (b) AlO_6, AO_9, and AO_{12} coordination polyhedra in $Ho_2SrAl_2O_7$.

[1] For communication IX, see [1].

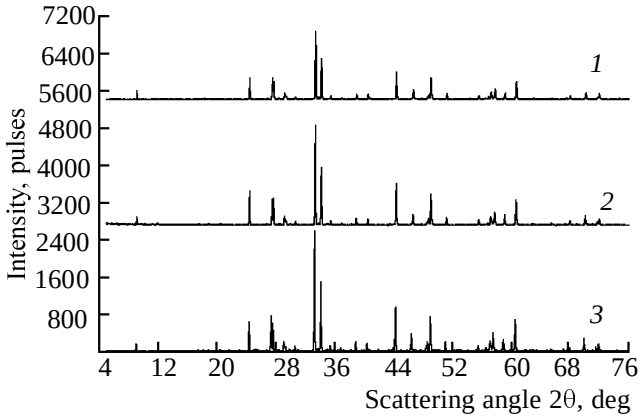

Fig. 2. X-ray diffraction patterns of $Ho_2SrAl_2O_7$ oxide at (*1*) 100, (*2*) 293, and (*3*) 673 K.

evidence for a substantially decreased distortion of all coordination polyhedra, which implied equalization of metal–oxygen bond lengths. Comparative analysis of the thermal expansion anisotropy of AO_9 polyhedra in P_2/RS and P/RS layered structures on the $Gd_2SrAl_2O_7$ and $YCaAlO_4$ (K_2NiF_4 structural type) oxides as examples revealed stronger equalization in the first case [10, 11]. The reason for this phenomenon is the existence of several coordination polyhedra—AO_{12}, AO_9, and AlO_6— linked into a single chain along the *c* axis of the structure (Fig. 1) (in the P/RS compounds, AO_9 and AlO_6). A competition seems to take place in metal–oxygen bond strengths, especially when octahedra join with nine-vertex polyhedra.

Table 1. Parameters *a* and *c* (Å) and volume *V* (Å^3) of the unit cell, atomic coordinates (*x*, *y*, *z*)[a], thermal parameters, *B* (Å^2), structural R_F and profile R_P divergence factors (%) for $Ho_2SrAl_2O_7$ at various temperatures

Parameter	100 K	293 K	693 K
a	3.7085(1)	3.7085(1)	3.7116(1)
c	19.4457(7)	19.4457(7)	19.5089(7)
V	267.386	267.386	268.91
	(Ho, Sr) × 2		
z	0.5	0.5	0.5
B	0.5(2)	0.7(4)	0.73(4)
	(Ho, Sr) ± 4		
z	0.3180(2)	0.3181(2)	0.3181(2)
B	0.68(13)	0.77(4)	0.76(9)
	Al × 4		
z	0.0950(10)	0.0960(7)	0.0957(8)
B	0.7(4)	0.91(4)	1.0
	O^1 × 2		
z	0	0	0
B	1.06(5)	2.0(1)	2.0
	O^2 × 8		
x	0.5	0.5	0.5
z	0.1100(10)	0.1019(7)	0.0989(8)
B	0.5(6)	0.5(4)	1.0
	O^3 × 4		
z	0.206(2)	0.207(1)	0.206(1)
B	0.9(9)	1.2(6)	1.0
R_F	5	7	8
R_P	16	19	19

[a] For all atoms, unless specified, *x* = *y* = 0.

This work presents the results of research into the changes in interatomic distances in the $Ho_2SrAl_2O_7$ oxide, that occur as the temperature increases from ambient to 673 K and decreases to 100 K. There have been no such studies on compounds of the $Ln_2SrAl_2O_7$ series at low temperatures. The compactness of $Ho_2SrAl_2O_7$ (owing to the lanthanide contraction) and large difference in the sizes of Ln^{3+} and Sr^{2+} cations made us to expect a still stronger anisotropy in changes in bond lengths in coordination tetrahedra in $Ho_2SrAl_2O_7$ compared with $Gd_2SrAl_2O_7$, up to appearance of contraction, viz. negative thermal expansion.

The X-ray diffraction patterns at three temperatures (Fig. 2) give evidence for the lack of structural changes in the range under study (100–673 K). At low temperatures, the crystal structure also does not change symmetry and still belongs to the *I*4/*mmm* space group. Comparative analysis of reflex intensities is difficult to perform because the X-ray diffraction patterns were recorded for different times. The differences in exposure time and step (at 100 K, the step is 0.04° at a constant count time of 14 s; at 293 and 673 K, the steps are 0.03° and 0.04°, respectively, at a count time of 20 s) are explained by limitations of the temperature control system.

The results of structural calculations (Rietveld refinement) for the three temperatures are given in Table 1. The experimental (I_{exp}), calculated (I_c), and difference X-ray patterns (for 298 K), obtained using the FULPROF program, are given in Fig. 3.

Figure 4 gives the plots of parameters and volume of the unit cell of $Ho_2SrAl_2O_7$ vs. temperature. The thermal expansion coefficient β, calculated on the assumption that the parameters vary linearly in the range from 100 to 673 K, is $\beta = 1/3(2\beta_a + \beta_c) = 2.5 \times 10^{-6}$ K^{-1} (β_a and β_c are the values of β along the *a* and *c* periods). This value is slightly lower than $\beta = 9 \times 10^{-6}$ K^{-1} for the isostructural aluminate $Gd_2SrAl_2O_7$ [10] and $\beta = 10^{-5}$ K^{-1} for the aluminate $YCaAlO_4$ [11], estimated in the range 293–1273 K.

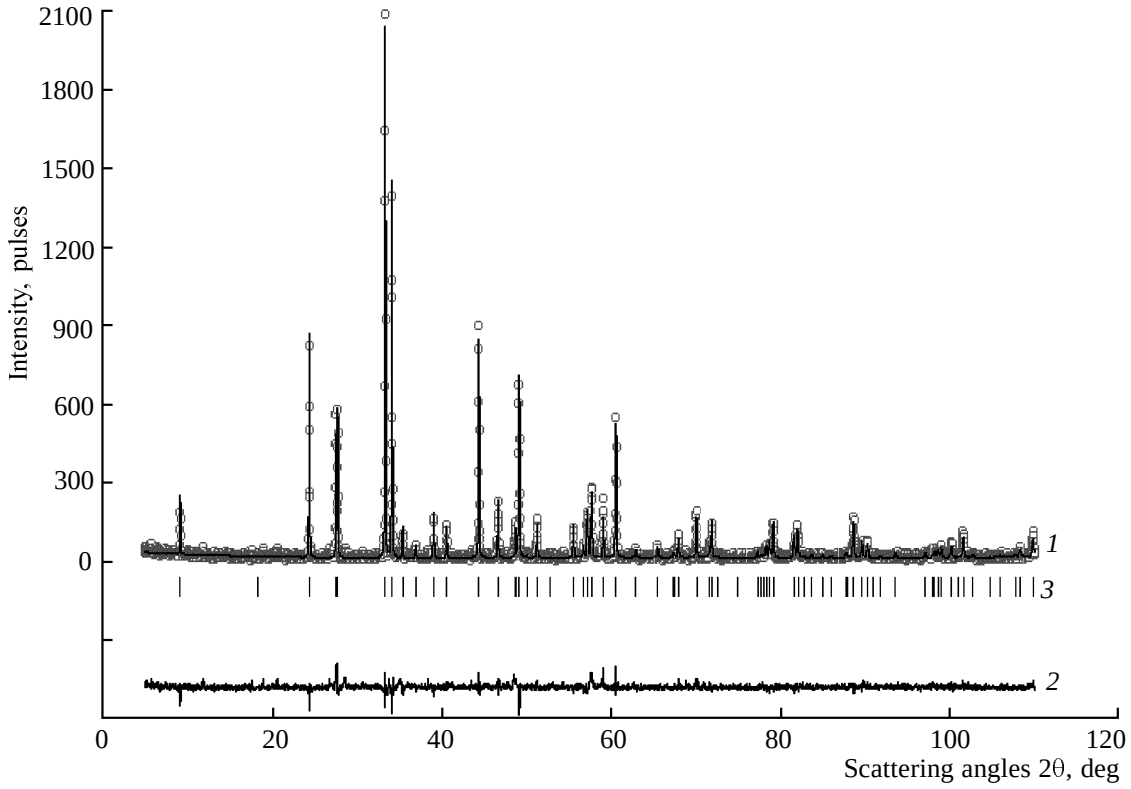

Fig. 3. (Circles) Experimental, (*1*) calculated, and (*2*) difference X-ray diffraction patterns and (*3*) positions of Bragg maxima for $Ho_2SrAl_2O_7$ as a function of scattering angle 2θ at 298 K.

The decrease of the thermal expansion coefficient can be explained by the fact that the unit cell parameters vary not strictly linearly and increase more and more rapidly as the temperature increases. These conclusions follow from Fig. 4. Since the structure of $Ho_2SrAl_2O_7$ was studied at lower temperatures and in a narrower temperature range, the observed increase in the *a* and *c* parameters with increasing temperature is less pronounced.

The current atomic coordinates *z* in unit cell period fractions are rather close for all the temperatures. The data in Table 1 show that the *z* coordinates for O^2 and Al get slightly closer to each other with increasing temperature, as is the case with $Gd_2SrAl_2O_7$. Aluminum atoms approach the plane of oxygen atoms as if they "enter" it, thus decreasing the distortion of the octahedron. The fact that the *z* coordinate for Ho^{+3} and Sr^{+2} remains almost unchanged, whereas that for Al^{+3} changes, is fully consistent with the stronger tendency of "lighter" for various kinds of displacements compared to "heavier" ones. However, this effect is less pronounced than in the $Gd_2SrAl_2O_7$ oxide that was studied at higher temperatures (293 and 1273 K) and in a wider temperature range. That is the reason why thermal vibrations of cations and oxygen atoms in $Ho_2SrAl_2O_7$ enhance not so essentially as the temperature increases.

The populations of structural sites by holmium and strontium atoms at all the three temperatures (Table 2) almost coincide with or are close to the values obtained at room temperature [4]. This result suggests that the cation distribution achieved in a 40-h synthesis at a higher temperature (1723 K) does not change during X-ray diffraction measurements (8–12 h) and that the results for the samples obtained at the same temperature in independent syntheses are

Table 2. Population of oxygen polyhedra in $Ho_2SrAl_2O_7$

T, K	AO_{12} cubic octahedron		AO_9 antiprism	
	HO^{+3}	Sr^{+2}	HO^{+3}	Sr^{+2}
100–673	0.22(2)	0.78(2)	0.89(2)	0.11(2)
298	0.18(2)	0.82(2)	0.91(2)	0.09(2)
Random distribution	0.67	0.33	0.67	0.33

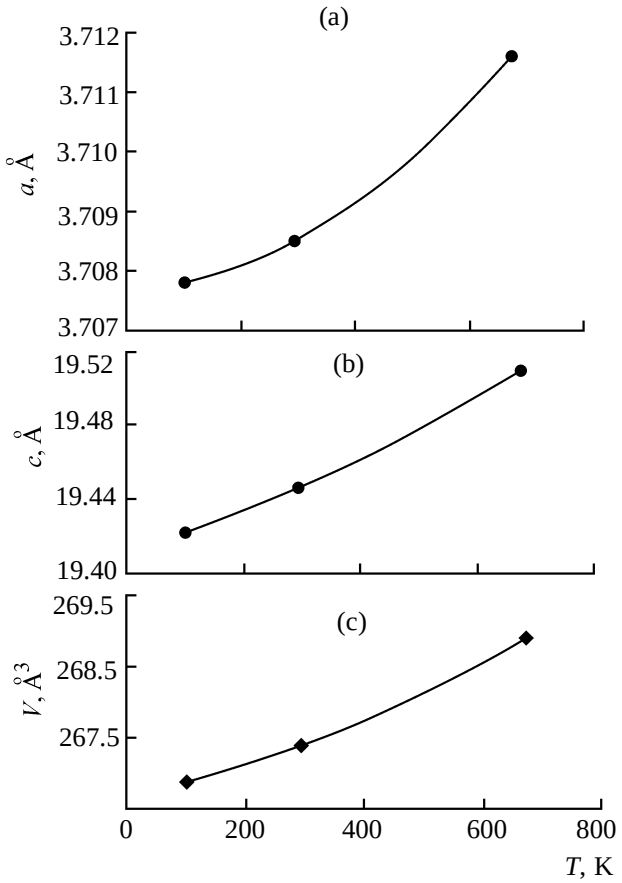

Fig. 4. Plot of the parameters (a) *a* and (b) *c* and (c) volume *V* of the unit cell of $Ho_2SrAl_2O_7$ vs. temperature.

Table 3. Interatomic distances (Å) and parameters Δ and α characterizing distortions of oxygen polyhedra in $Ho_2Sr \cdot Al_2O_7$ (A = Ho, Sr)

Parameter	100 K	293 K	673 K
AO_{12} cubic octahedron			
$A–O^1 \times 4$	2.6216(2)	2.622(1)	2.625(1)
$A–O^2 \times 8$	2.828(15)	2.714(10)	2.677(11)
Δ(A–O)	0.21(2)	0.09(1)	0.05(1)
AO_9 antiprism			
$A–O^3 \times 1$	2.18(3)	2.15(3)	2.18(3)
$A–O^3 \times 4$	2.661(5)	2.670(5)	2.668(5)
$A–O^2 \times 4$	2.322(12)	2.420(9)	2.463(11)
Δ(A–O^3 and A–O^2)	0.34(2)	0.25(1)	0.20(2)
AlO_6 octahedron			
$Al–O^3 \times 1$	2.15(4)	2.17(3)	2.16(3)
$Al–O^1 \times 1$	1.88(1)	1.87(1)	1.87(1)
$Al–O^2 \times 4$	1.84(2)	1.858(1)	1.857(1)
α_1 = Al–O^3/Al–O^1	1.15	1.16	1.16
α_2 = Al–O^1/Al–O^2	1.02	1.00	1.00
α_3 = Al–O^3/Al–O^2	1.17	1.16	1.16

reproducible. A deviation from disordered distribution is observed in the case of $Ho_2SrAl_2O_7$ oxide where $(Ho,Sr)O_9$ antiprisms are preferentially occupied by holmium cations and $(Ho,Sr)O_{12}$ cubic octahedral, by strontium cations. Such distribution is accounted for by the difference in the ionic radii of Ho^{+3} and Sr^{+2} cations {for the nine-coordinated state $R(Ho^{+3})$ 1.07 and $R(Sr^{+2})$ 1.31 Å [12]} and by the tendency of the smaller holmium cations to occupy the smaller AO_9 polyhedra. On the whole we observe a distribution close to complete ordering of holmium cations in the RS layer and of strontium cations in the P layer. The tendency for positional ordering in the $Ln_2SrAl_2O_7$ oxides enhances in the Ln–Ho series was described in detail in [4, 9]. The positional ordering of alkaline-earth and rare-earth metal cations takes place also in the case of isomorphic isovalent substitution of calcium for strontium in $Ln_2SrAl_2O_7$ (Ln = La, Nd) [13,14], when the smaller Ca^{+2} cation prefers to occupy nine-vertex oxygen polyhedra.

The interatomic distances in the coordination polyhedra and their temperature variations are given in Table 3. Examination of these values establishes the following. First, there is a substantial anisotropy of interatomic interactions in all the polyhedra, the greatest difference in bond lengths Δ(A–O) at all the temperatures is observed in the $(Ho,Sr)O_9$ antiprism and the smallest, in the $(Ho,Sr)O_{12}$ cubic octahedra. Second, not all bond lengths increase with temperature. The most affected are $A–O^2$ interatomic distances: Eight bonds in the AO_{12} cubic octahedra shorten and four bonds in the AO_9 antiprism lengthen. Therewith, the $Al–O^2$ equatorial bond lengthens moderately, which at first sight seems inconsistent with increase in the *a* parameter. This occurs just because aluminum atoms in the octahedra are shifted from the plane of the equatorial O^2 atom to the axial O^1 atom, as evidenced by the difference in the *z* coordinates for Al and O^2 (Table 1). As the temperature increases, O^2 approaches the plane of aluminum atoms, the AlO_2Al angle decreases, and the length of equatorial AlO^2 bonds slightly increases. The character of octahedron distortion is almost invariable in the temperature range under study, which follows from the tetragonal distortion coefficients α_1–α_3 (Table 3). The length of the bridging A–O^-–Al bond remains almost insensitive to temperature.

The results of this study show that $Ln_2SrAl_2O_7$ cannot be assigned to compounds with negative thermal expansion, since all parameters and the volume of the unit cell by and large increase. They also do not belong to compounds with anisotropy of thermal expansion, whose unit cell parameters characteristically differently increase with temperature.

At the same time, layered oxides of the $Ln_2SrAl_2O_7$ series are of obvious interest owing to the anisotropy of thermal expansion of the coordination polyhedra located in various layers of the perovskite-like layered structure. The anisotropy of interatomic interactions in the coordination polyhedra results, in force of special features of their formation from polyhedra of various structural types, in that, as the temperature increases, the polyhedra expand in a number of directions, while in certain cases they contract. Hence, for the $Ho_2SrAl_2O_7$ compound we can speak about "negative" expansion at a microlevel within the unit cell. In the same sense, we can speak about anisotropy of thermal expansion.

Thus, the layered structural type introduces specific features in the phenomenon of thermal expansion of a substance, which can also affect thermophysical properties that depend on the character of the nearest surrounding and on the distortion of the structure as a whole.

EXPERIMENTAL

The $Ho_2SrAl_2O_7$ complex oxide was synthesized by the ceramic procedure from holmium oxide (SST brand, main component content 99.99%), finely dispersed aluminum oxide (Johnson Matthey 99.99%, grain size 1–15 μm), and strontium carbonate (special purity grade 7–2, Technical Specifications 6-09-01-659-91), taken in proportions corresponding to the following equation of the synthesis.

$$Ho_2O_3 + Al_2O_3 + SrCO_3 = Ho_2SrAl_2O_7 + CO_2.$$

The batch thoroughly mixed in an agate mortar was pressed into pellets 0.5 g in weight and 0.7 cm in diameter and sintered in corundum crucibles in air for 40 h at 1723 K in a silite furnace. The temperature was controlled with a platinum–rhodium thermocouple. The isothermal regime of thermal treatment was maintained with an accuracy of ±1°C (TP 403 programmed thermocontroller).

The X-ray diffraction patterns were recorded on a Bruker-AXS diffractometer in a thermally controlled chamber in the $5° < 2\theta < 110°$ range at 100 (step 0.04°, constant count time 14 s), 293 (step 0.03°, constant count time 20 s), and 673 K (step 0.04°, constant count time 20 s).

The unit cell parameters and interatomic distances were determined in the *I*4/*mmm* space group from full-profile X-ray diffraction patterns with subsequent Rietveld refinement [15, 16].

ACKNOWLEDGMENTS

The work was financially supported by the Russian Foundation for Basic Research (project no. 04-03-32176) and *Universities of Russia* Program (project no. UR.06.01.02).

REFERENCES

1. Smirnov, Yu.E., Smirnova, T.D., and Zvereva, I.A., *Russ. J. Gen. Ghem.*, 2005, vol. 75, no. 9, p. 1359.
2. Fava, J. and Le Flem, G., *Mat. Res. Bull.*, 1975, vol. 10, no. 1, p. 75.
3. Udalov, Yu.P., Salmon, P., and Bondar', I.A., *Zh. Neorg. Khim.*, 1976, vol. 21, no. 2, p. 541.
4. Zvereva, I., Smirnov, Yu., Gusarov, V., Popova, V., and Choisnet, J., *Solid State Sci.*, 2003, vol. 5, no. 2, p. 343.
5. Zvereva, I.A., Popova, V.F., Vagapov, D.A., Toikka, A.M., and Gusarov, V.V., *Russ. J. Gen. Chem.*, 2001, vol. 71, no. 8, p. 1181.
6. Zvereva, I.A., Popova, V.F., Pylkina, N.S., and Gusarov, V.V., *Russ. J. Gen. Chem.*, 2003, vol. 73, no. 1, p. 43.
7. Zvereva, I.A., Popova, V.F., Missyul', A.B., Toikka, A.M., and Gusarov, V.V., *Russ. J. Gen. Chem.*, 2003, vol. 73, no. 5, p. 684.
8. Ruddlesden, S.N. and Popper, P., *Acta Crystallogr., Sect. A*, 1958, vol. 11, no. 1, p. 54.
9. Zvereva, I.A., Smirnov, Yu.E., Vagapov, D.A., and Choisnet, J., *Zh. Obshch. Khim.*, 2000, vol. 70, no. 12, p. 1957.
10. Zvereva, I.A., Smirnov, Yu.E., and Choisnet, J., *Russ. J. Gen. Chem.*, 2004, vol. 74, no. 5, p. 655.
11. Choisnet, J., Archaimbault, F., Crespin, M., Chezhina, N., and Zvereva, I., *Eur. Solid State Inorg. Chem.*, 1993, vol. 30, no. 4, p. 619.
12. Shannon, R.D., *Acta Crystallogr., Sect. A*, 1976, vol. 32, no. 5, p. 751.
13. Zvereva, I., Smirnov, Yu., and Choisnet, J., *Int. J. Inorg. Mater.*, 2001, vol. 3, no. 1, p. 95.
14. Zvereva, I.A., Seitablaeva, S.R., and Smirnov, Yu.E., *Russ. J. Gen. Chem.*, 2003, vol. 73, no. 1, p. 31.
15. Rietveld, H., *Appl. Crystallogr.*, 1969, vol. 2, no. 1, p. 65.
16. Rodriguez-Carvajal, J.L., *Physica B*, 1992, vol. 192, no. 1, p. 55.